

Supporting Information

Carbazole-based fully conjugated sp^2 c D-A Covalent Organic polymer for Visible Light Mediated Photocatalytic degradation of Rhodamine B and Rose Bengal

*Kamal Verma, K. R. Justin Thomas**

Organic Materials Laboratory, Department of Chemistry, Indian Institute of Technology
Roorkee, Roorkee – 247667, India.

School of Science and Technology, Nottingham Trent University, Nottingham NG11 8NS,
U.K.

*Corresponding author. E-mail: krjt@cy.iitr.ac.in

Table of contents

1. General Information
2. Synthesis and general procedure
3. Experimental setup
4. Characterizations
5. Spectroscopic characterization
6. Comparison table
7. References
8. NMR data
9. MALDI-TOF Mass Characterization.

1. GENERAL INFORMATION

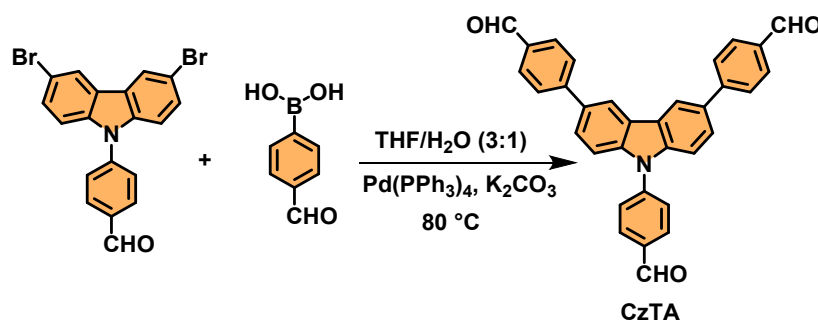
Carbazole (98%) and 1,4-phenylenediacetonitrile (98%) were purchased from Avra chemicals. Dioxane (99%, extra pure) was purchased from Sd- fine chemicals, and mesitylene (99%) was purchased from fisher scientific. For the application part, Rhodamine B and Rose Bengal was purchased from commercial sources. The analytical grade solvents and commercially available reagents were purchased from SDFCL, AVARICE, Fisher Scientific, MERCK, THOMAS BAKER, Spectrochem, AVRA, and LOBA Chemie. All the purchased reagents were used without further purification. Non-commercially available starting materials were synthesized by known literature procedures and their physical and spectroscopic data were compared with the reported values. Progress of the reactions was measured by thin-layer chromatography (TLC) on pre-coated aluminium backed plates. Purification of the derivatives was done by column chromatography on Silica gel (100-200 mesh sizes well as 200-400 mesh size). NMR spectra were acquired on a BRUKER 500 MHz spectrometer for ^1H and ^{13}C respectively. Chemical shifts (δ) are reported in ppm relative to residual solvent signals (CDCl_3 : 7.26 ppm for ^1H NMR and 77.16 ppm for ^{13}C NMR/ DMSO-d_6 : 2.50 ppm for ^1H NMR and 39.52 ppm for ^{13}C NMR). ^{13}C NMR spectra were acquired on a broadband decoupled mode. The following abbreviations are used to describe peak patterns: s (singlet), d (doublet), t (triplet), q (quartet), quint (quintet), sept (septuplet), m (multiplet), dd (doublet of doublet) br s (broad singlet). Bruker AXS D8 Advance diffractometer, which was set to 40 kV and 30 mA, was employed for the acquisition of PXRD data. Monochromatized Cu $K\alpha$ radiation was used, and the data was collected within the angular range of $2\text{--}40^\circ$ with a step size of 0.02° . ^1H and ^{13}C NMR spectra were recorded on BRUKER 500 MHz spectrometer respectively. To analyze the microstructure, Carl Zeiss FE-SEM, ultra plus 55 equipped with Energy dispersive X-ray spectroscopy (EDS) (oxford instruments) was used. It was operated at an accelerating voltage of 20 kV. For the sample preparation, the sample was affixed on metal stub using carbon tape.

Gold coating was applied using a sputter unit with 50 μ A current for 90s to prevent charging. Silver paste was applied to ensure the conductivity of the sample. To ascertain the elemental composition area analysis was carried out in different regions. Specific surface area analysis of the compounds was carried out on NovaWin, Quantachrome instrument using Brunauer-Emmett-Teller (BET) method. UV-Vis Diffuse Reflectance spectroscopy (UV- Vis DRS) measurement was carried out on Shimadzu 2450 UV-Vis spectrophotometer in the range 200-800 nm to find the band gap of the material. For that material was mixed with reference material BaSO₄ and pelletized. For the determination of oxidation state of the elements present in the material PHI 5000 Versa Probe III X-ray Photoelectron Spectrometer (XPS) with Al-K α X-ray source ($h\nu = 1486.6$ eV) was used. C 1s peak was taken as the reference peak for binding energy correction and MULIPAK software was used for the analysis of binding energy. For the calculation of valence band maxima of the materials, Ultraviolet Photoelectron Spectroscopy (UPS) measurement of the compounds was carried out using PHI 5000 Versa Probe III. For that monochromatic He I light source (21.22 eV) was used. The photochemical reaction was perform in 30W white CFL light.

Electrochemical characterization. For the Mott – Schottky measurement of the compounds, the Metrohm electrochemical workstation (Multi Autolab/M204) was used. Three electrode systems were used for the measurement in which Pt wire act as working electrode, Ag/AgCl electrode functions as reference electrode and material deposited Indium Tin Oxide (ITO) glass electrode act as the working electrode. Two electrode systems were used for the measurement in which Pt wire acts as a counter electrode and material deposited ITO as working electrode. Sample preparation was done by dispersing the mixture of the compound and binder polyvinylidene fluoride (PVDF) in 90:10 ratio in *N*-methylpyrrolidone (NMP) solvent. This mixture was placed on stirrer for few hours to make a fine slurry and deposited on ITO glass of dimension 1 cm \times 2 cm. 0.1M Na₂SO₄ was used for the Mott-Schottky measurement.

2. Synthesis and general procedures

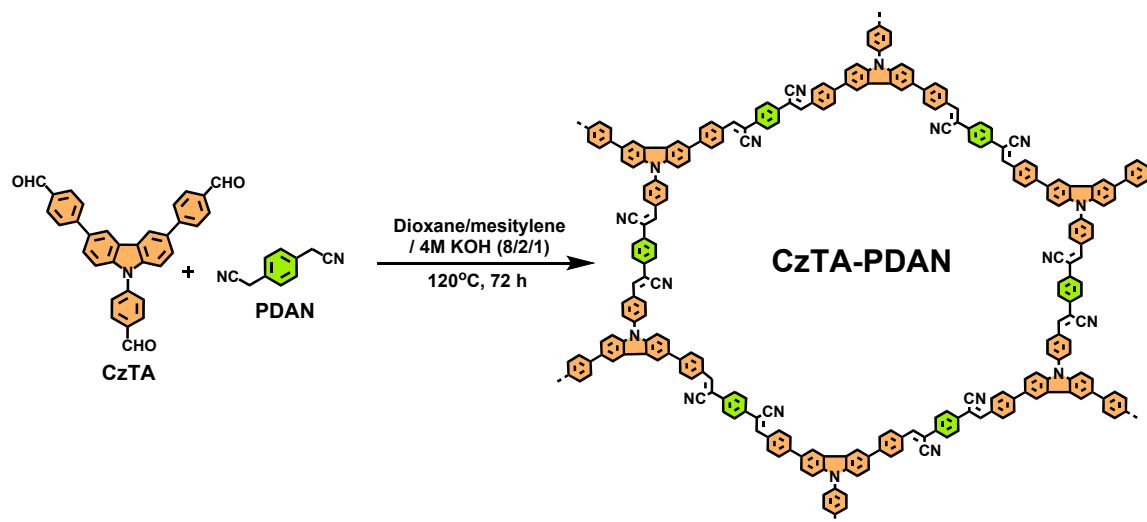
2.1. 4,4',4''-(9*H*-carbazole-3,6,9-triyl)tribenzaldehyde (CzTA). A mixture of 4-(3,6-Dibromo-9*H*-carbazole-9-yl)-benzaldehyde (1 g, 2.33 mmol), 4-formylphenylboronic acid (0.82 g, 5.83 mmol/2.5 equiv.), Pd(PPh₃)₄ (5 mol%) and K₂CO₃ (2.25 g, 16.31 mmol/ 7 equiv.) was taken into a two neck RB and purge nitrogen for 15 minute after purging add degassed THF:H₂O into it. Now the mixture was heated to 80°C. The progress of the reaction was monitored by TLC. After 24 h, the starting materials disappeared indicating the completion of the reaction. The reaction was quenched by the addition of ice water. The solid precipitate of the organic product was filtered. The collected solid was washed with ethyl acetate several times and dried under a vacuum oven. The isolated yield of the final product was obtained 72%. ¹H NMR (500 MHz, CDCl₃) δ 10.17 (s, 1H), 10.09 (s, 2H), 8.49 (s, 2H), 8.21 (d, *J* = 8.2 Hz, 2H), 8.02 (d, *J* = 8.0 Hz, 4H), 7.91 (d, *J* = 8.0 Hz, 4H), 7.86 (d, *J* = 8.3 Hz, 2H), 7.78 (d, *J* = 7.7 Hz, 2H), 7.62 (d, *J* = 8.5 Hz, 2H).



Scheme S1. Synthesis of the 4,4',4''-(9*H*-carbazole-3,6,9-triyl)tribenzaldehyde (CzTA).

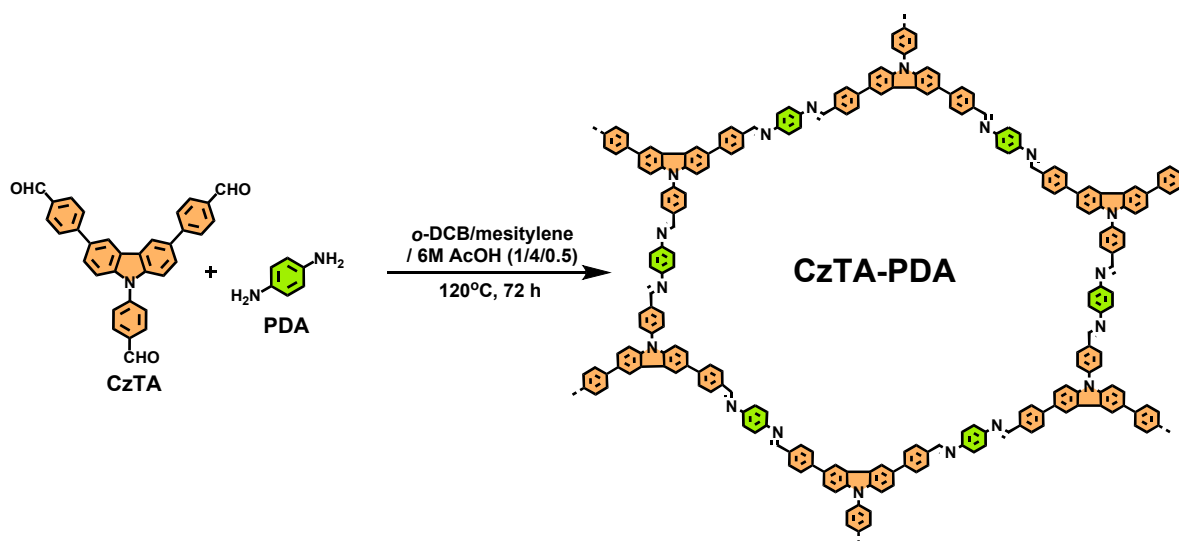
2.2. Synthesis of CzTA-PDAN COP. Phenylenediacetonitrile (0.45 mmol, 70 mg) and 4,4',4''-(9*H*-carbazole-3,6,9-triyl)tribenzaldehyde (0.30 mmol, 145 mg) were taken in a sealed tube and add a mixture of *o*-DCB/Mesitylene (0.8/3.2 mL, *v/v* 1/4) and 6M acetic acid (0.4 mL) into it and sonicated for five minutes. Now degassed via the freeze-pump-thaw process. Then the tube was sealed and allowed the reaction for 3 days at 120 °C. The precipitate is collected,

washed with suitable solvents, and dried under vacuum to yield the COP (isolated yield 87%) as yellow solid powder.



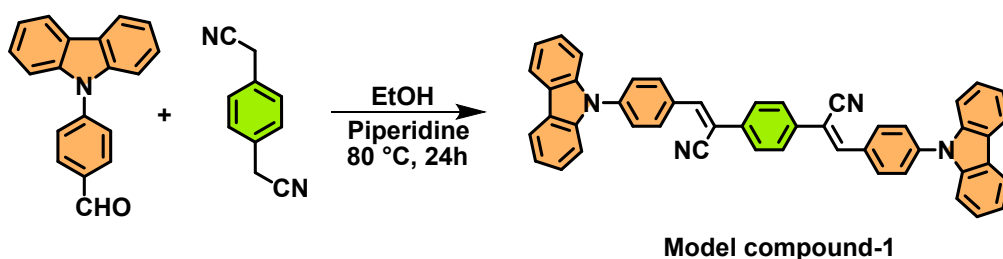
Scheme S2. Synthesis of CzTA-PDAN COP.

2.3. Synthesis of CzTA-PDA COP. Phenylenediamine (0.45 mmol, 48 mg) and 4,4',4''-(9H-carbazole-3,6,9-triyl)tribenzaldehyde (0.30 mmol, 145 mg) was taken in a seal tube and add mixture of *o*-DCB/Mesitylene(0.8/3.2 mL, *v/v* 1/4) and 6M acetic acid (0.4 mL) into it and sonicated for five minute. Now degassed via freeze-thaw process. Then the tube was sealed and allowed the reaction for 3 days at 120°C. The precipitate is collected, washed with suitable solvents, and dried under vacuum to yield the COP (isolated yield 95%) as yellow solid powder.



Scheme S3. Synthesis of CzTA-PDA COP.

2.4. Synthesis of Model compound-1. A mixture of 4-(9*H*-carbazole-9-yl)-benzaldehyde (1 g, 2.33 mmol), Phenylenediacetonitrile (25 mg, 0.071 mmol) was taken into a single neck RB, add EtOH/piperidine (10 mL/1 mL) into it. Now the mixture was heated to 80°C. The progress of the reaction was monitored by TLC. After 24 h, the starting materials disappeared indicating the completion of the reaction. The solid product was filtered. Now, the residue solid was washed with EtOH and dried in a vacuum oven at 70°C for 3h, giving a light-yellow residue. The isolated yield of the final product was obtained 68%. ¹H NMR (500 MHz, DMSO-*D*₆) δ 10.03 (s, 2H), 8.54 (d, *J* = 8.6 Hz, 4H), 8.30 – 8.10 (m, 7H), 8.09 – 7.92 (m, 14H), 7.65 – 7.50 (m, 7H), 7.43 (t, *J* = 7.6 Hz, 3H), 7.17 (t, *J* = 7.4 Hz, 3H), 7.07 (dd, *J* = 12.0, 5.0 Hz, 5H), 4.45 (t, *J* = 7.1 Hz, 6H), 1.82 – 1.66 (m, 6H), 1.38 – 1.22 (m, 6H), 0.90 – 0.76 (m, 9H).



Scheme S4. Synthesis of Model compound-1.

3. EXPERIMENTAL SETUP

2 × 18 W CFL light bulbs were attached at both sides of a magnetic stir. The distance between the two light bulbs was 14 cm. The reaction was carried out in a 30 mL borosilicate glass vial with a magnetic bar. During the reaction, the distance of CFL lights from the borosilicate glass vials was kept at 6 cm and the temperature was maintained at room temperature (20-25 °C) with air cooling.

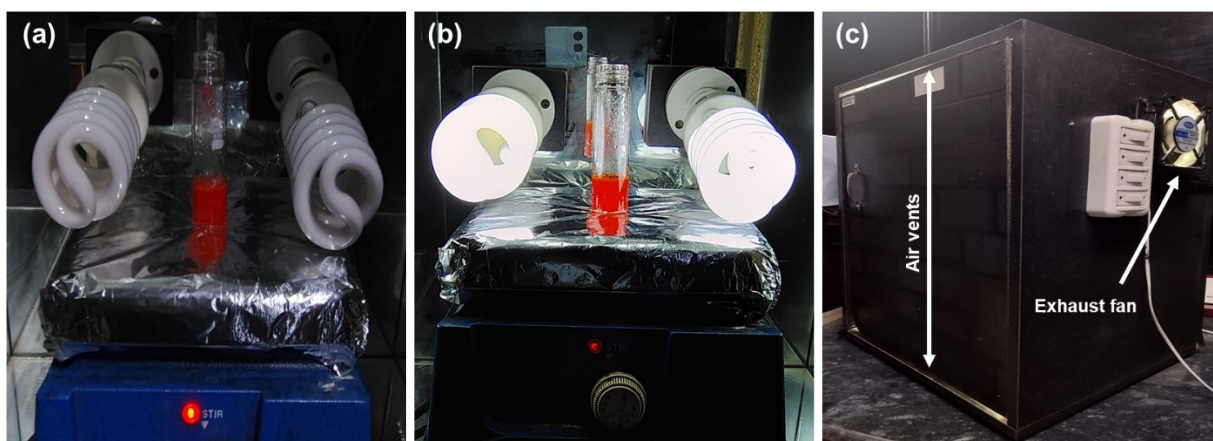


Figure S1. A photochemical reaction set up for photocatalytic dye degradation; (a) Light off, (b) Light on, (c) Photoreactor.

4. CHARACTERIZATIONS

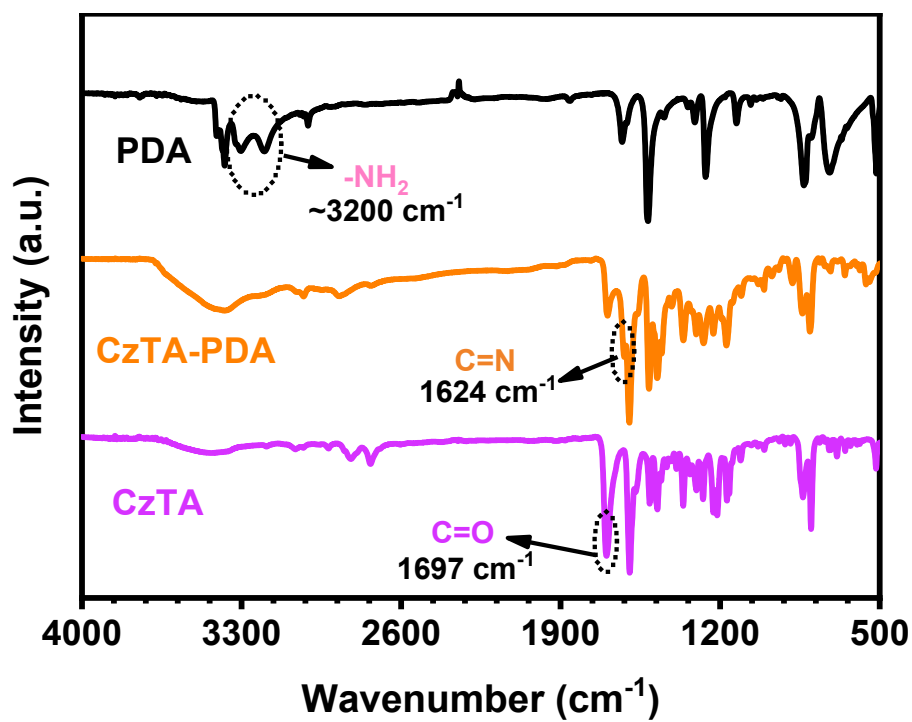


Figure S2. FT-IR spectra of the CzTA-PDA COP.

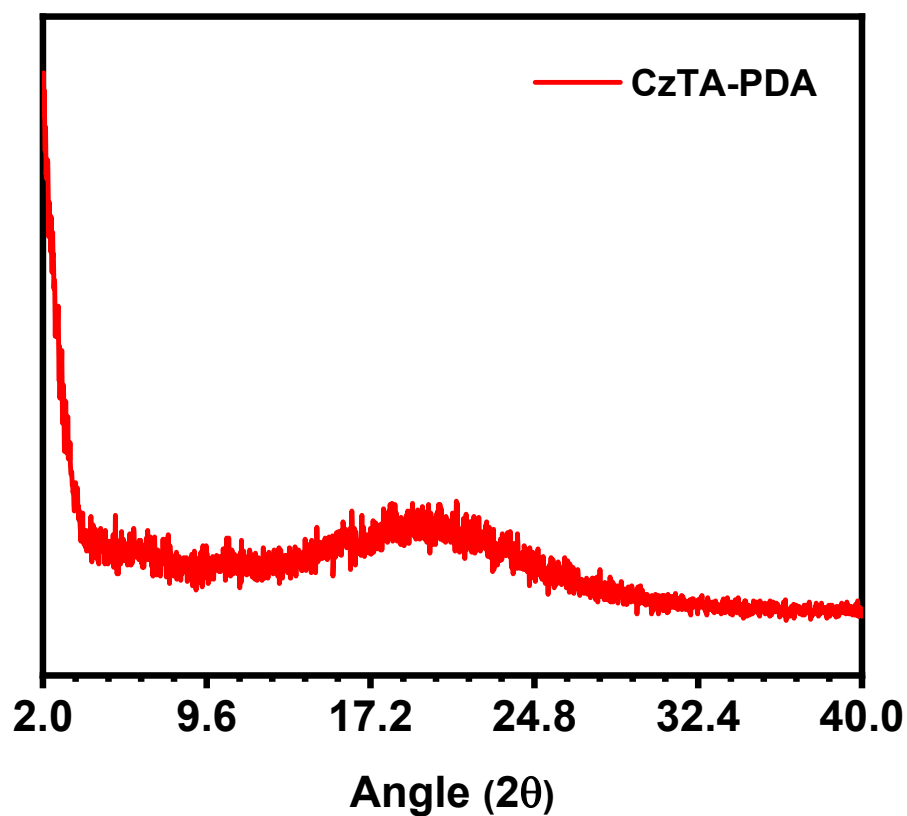


Figure S3. Experimentally observed PXRD pattern of CzTA-PDA COP.

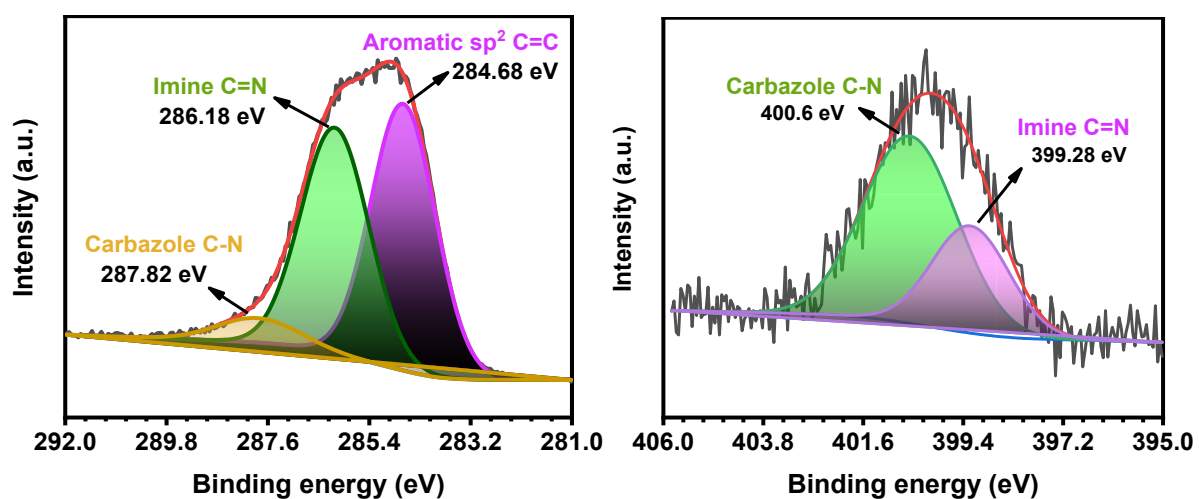


Figure S4. (a) High-resolution $C1s$ XPS spectrum, (b) High-resolution $N1s$ XPS spectrum, of CzTA-PDA COP.

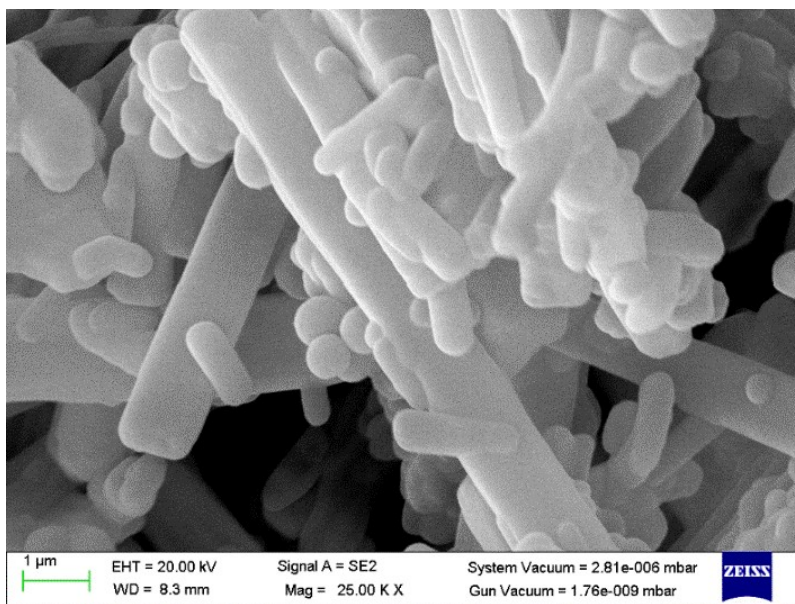


Figure S5. SEM images of CzTA-PDA COP.

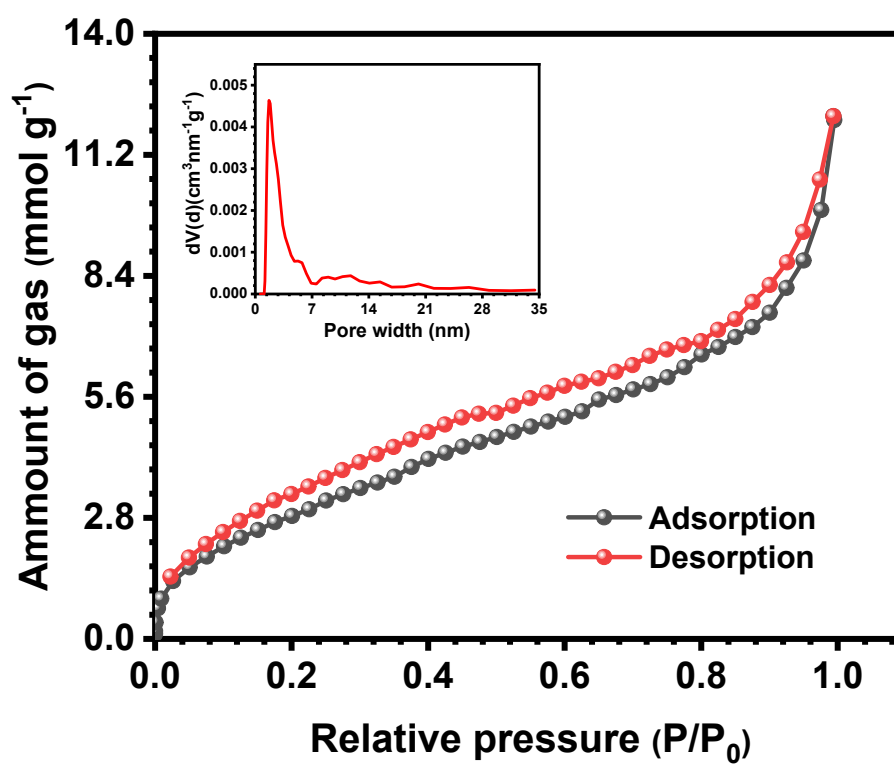


Figure S6. N₂ isotherm of the CzTA-PDA COP at 77 K, inset: pore width distribution of the CzTA-PDA COP.

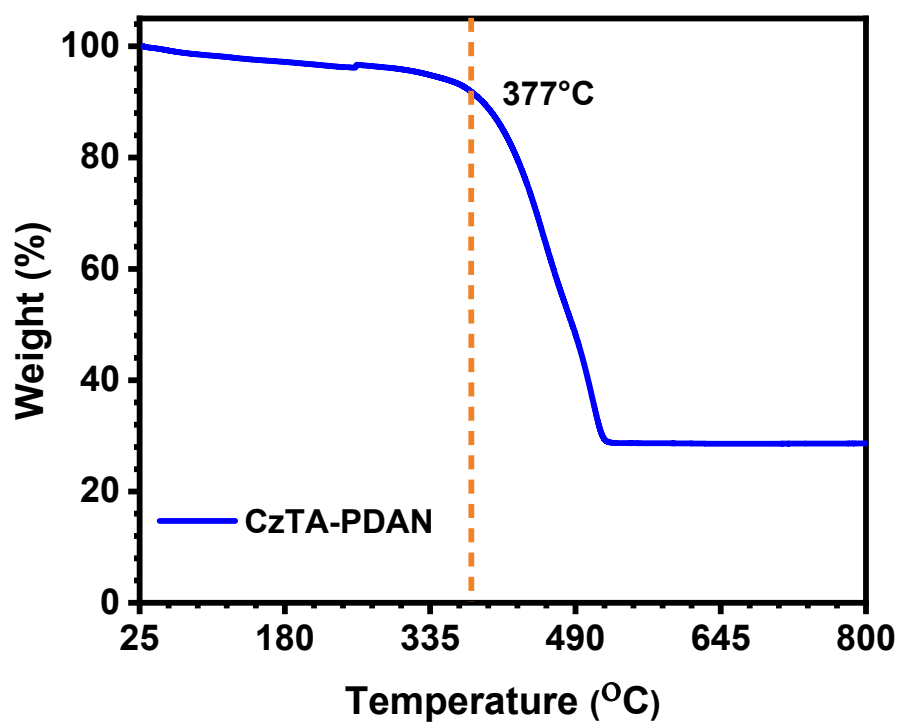


Figure S7. TGA curve of the CzTA-PDAN COP under oxygen atmosphere.

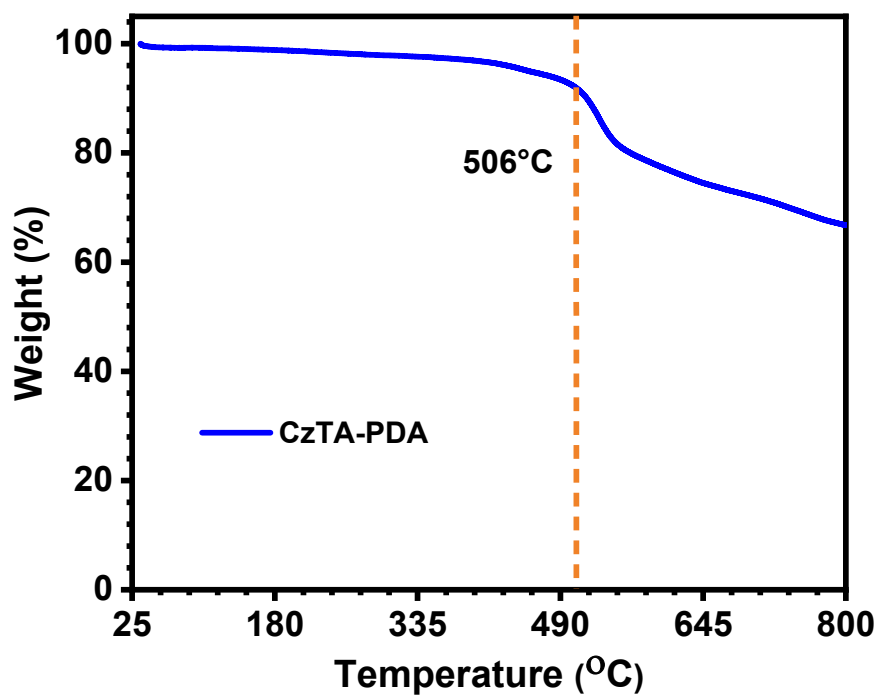


Figure S8. TGA curve of the CzTA-PDA COP.

5. SPECTROSCOPIC CHARACTERIZATION

5.1. Photocatalytic degradation study at different pH for Rhodamine B (RhB)

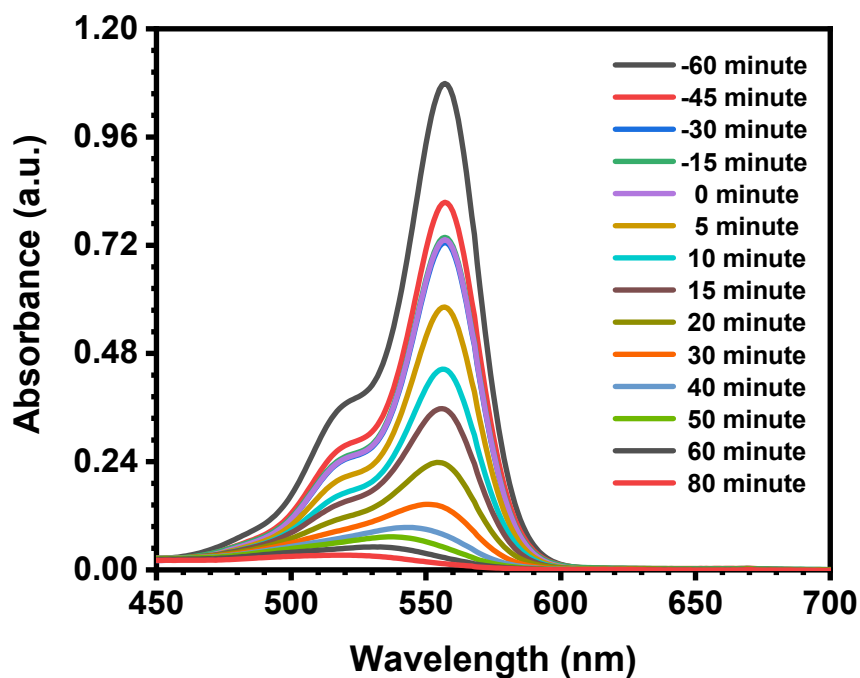


Figure S9. Photocatalytic degradation of RhB at pH 2 catalyzed by CzTA-PDAN COP.

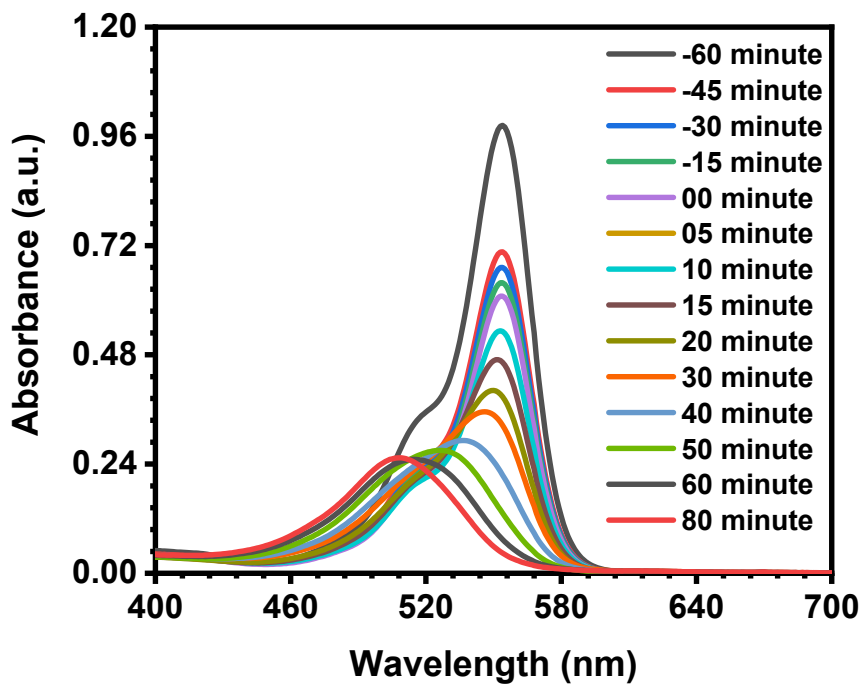


Figure S10. Photocatalytic degradation of RhB at pH 5 catalyzed by CzTA-PDAN COP.

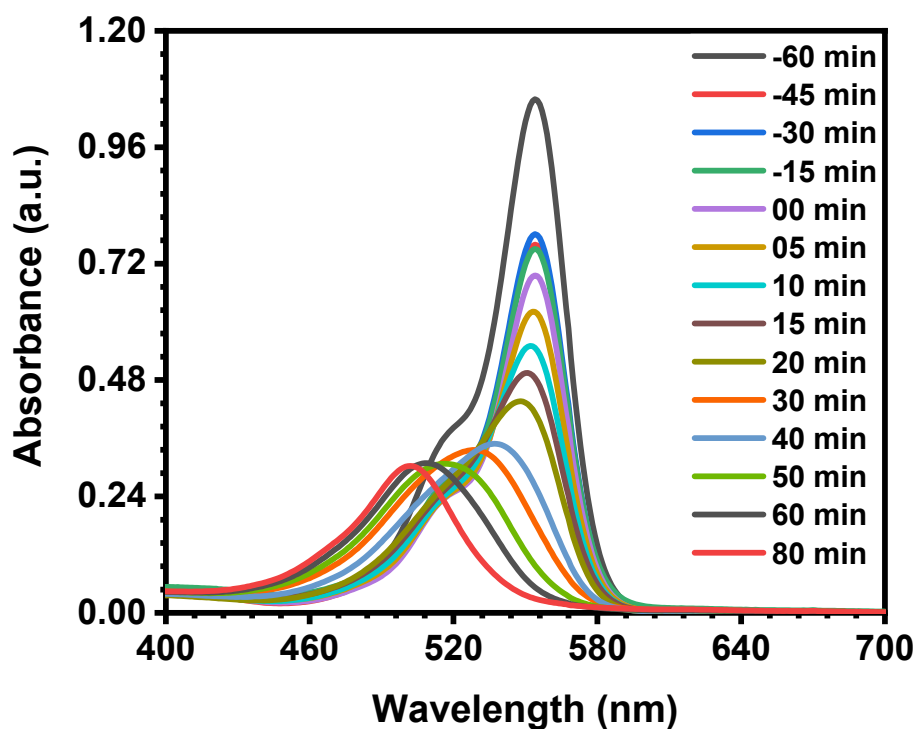


Figure S11. Photocatalytic degradation of RhB at pH 7 catalyzed by CzTA-PDAN COP.

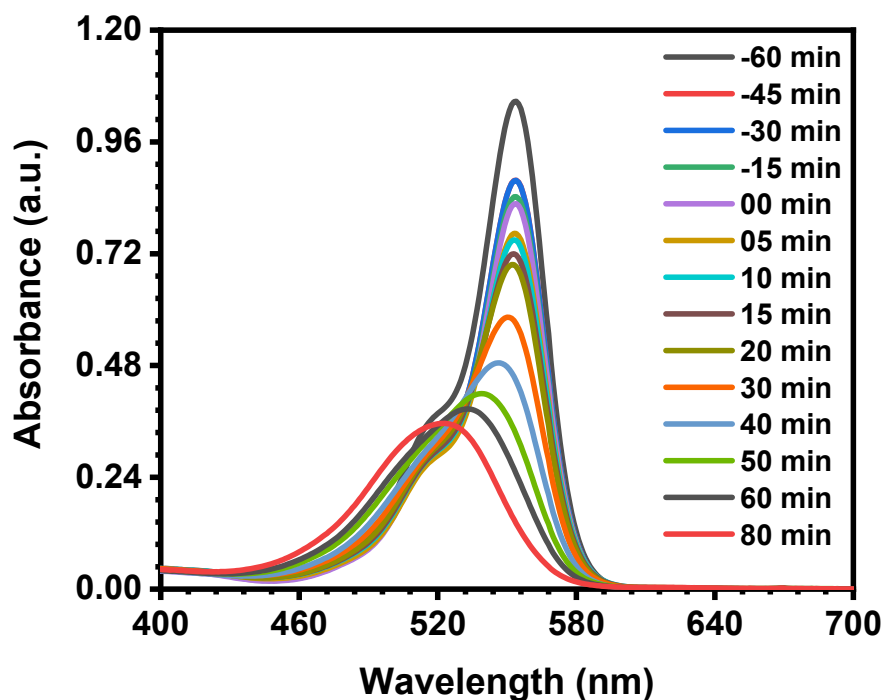


Figure S12. Photocatalytic degradation of RhB at pH 7 catalyzed by CzTA-PDAN COP.

5.2. Photocatalytic degradation study at pH 2 for Rhodamine B (RhB) with different scavengers

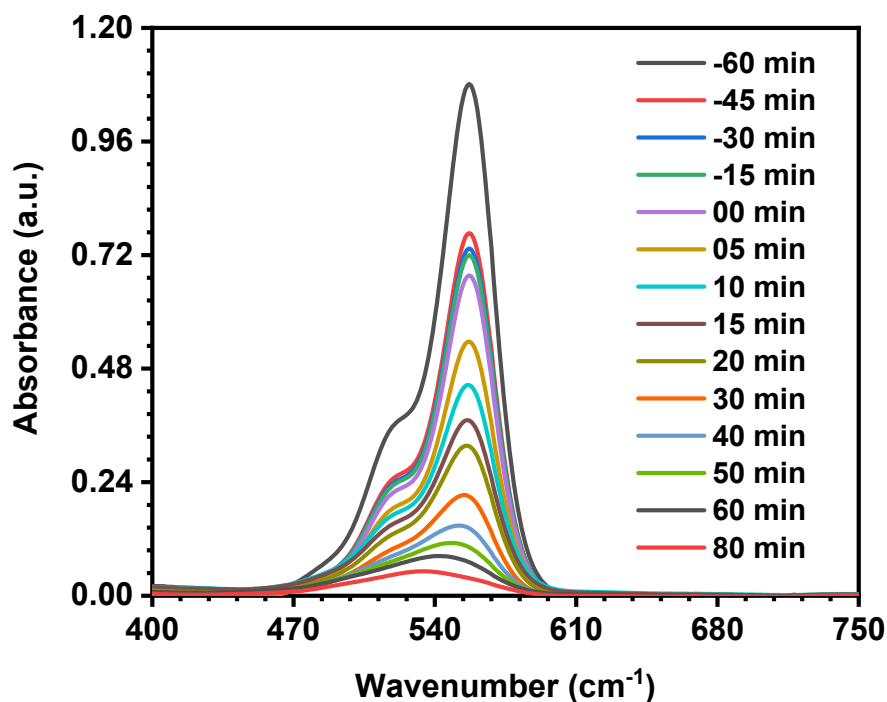


Figure S13. Photocatalytic degradation of RhB at pH 2 catalyzed by CzTA-PDAN COP in presence of isopropyl alcohol (IPA) as hydroxyl radical scavenger.

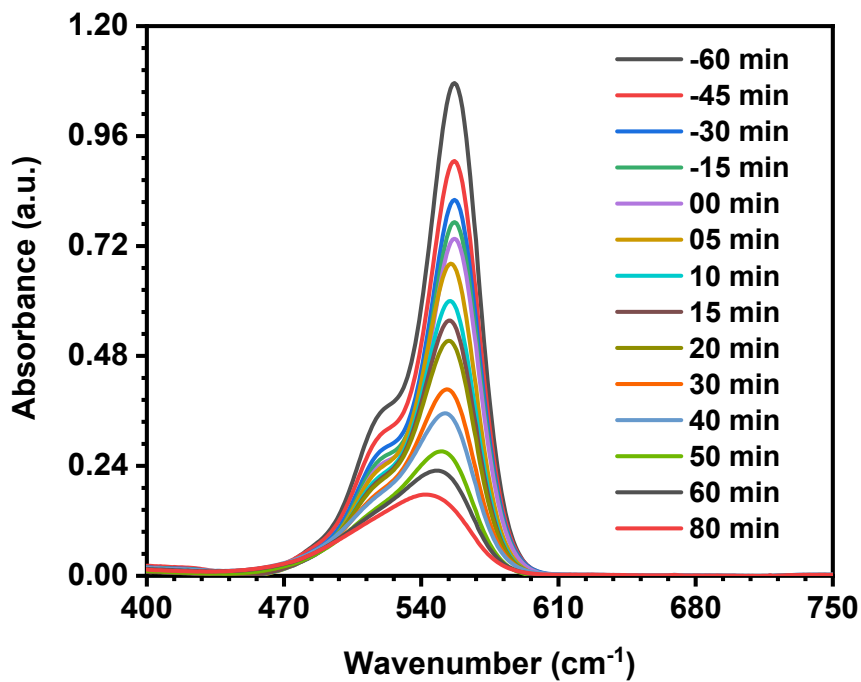


Figure S14. Photocatalytic degradation of RhB at pH 2 catalyzed by CzTA-PDAN COP in presence of ammonium oxalate (AO) as holes scavenger.

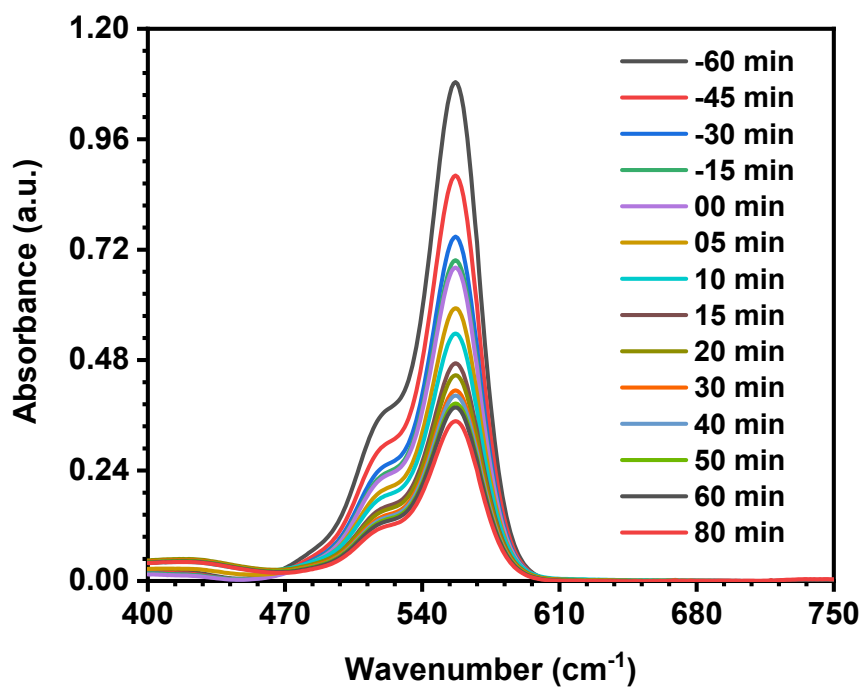


Figure S15. Photocatalytic degradation of RhB at pH 2 catalyzed by CzTA-PDAN COP in presence of benzoquinone (BQ) as superoxide radical anion scavenger.

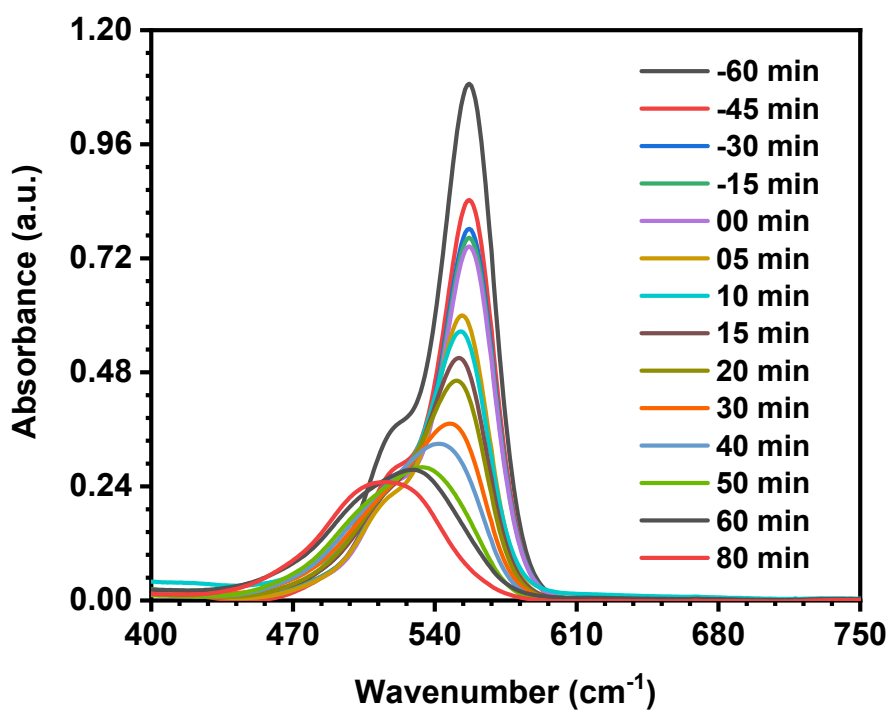


Figure S16. Photocatalytic degradation of RhB at pH 2 catalyzed by CzTA-PDAN COP in the presence of sodium azide (NaN_3) as a singlet oxygen scavenger.

5.3. Photocatalytic degradation study at pH 2 for Rose Bengal (RB) with different scavengers

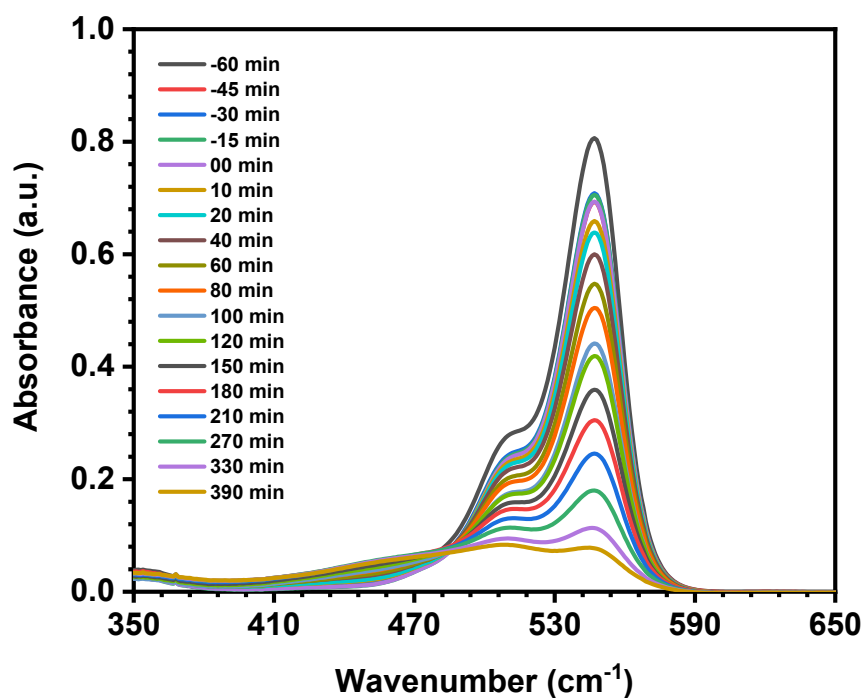


Figure S17. Photocatalytic degradation of RB at pH 7 catalyzed by CzTA-PDAN COP in presence of isopropyl alcohol (IPA) as hydroxyl radical scavenger.

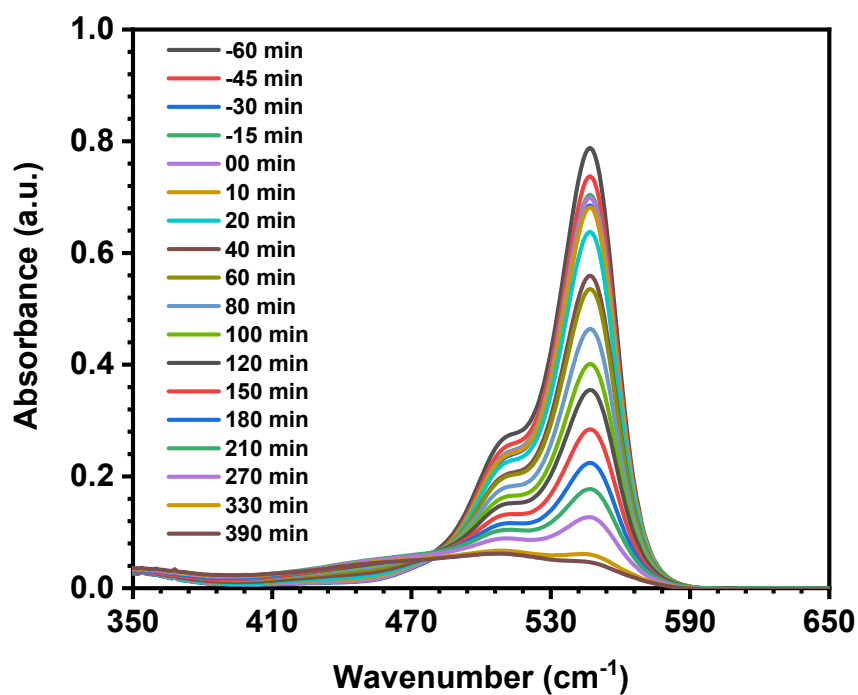


Figure S18. Photocatalytic degradation of RB at pH 7 catalyzed by CzTA-PDAN COP in presence of ammonium oxalate (AO) as hole scavenger.

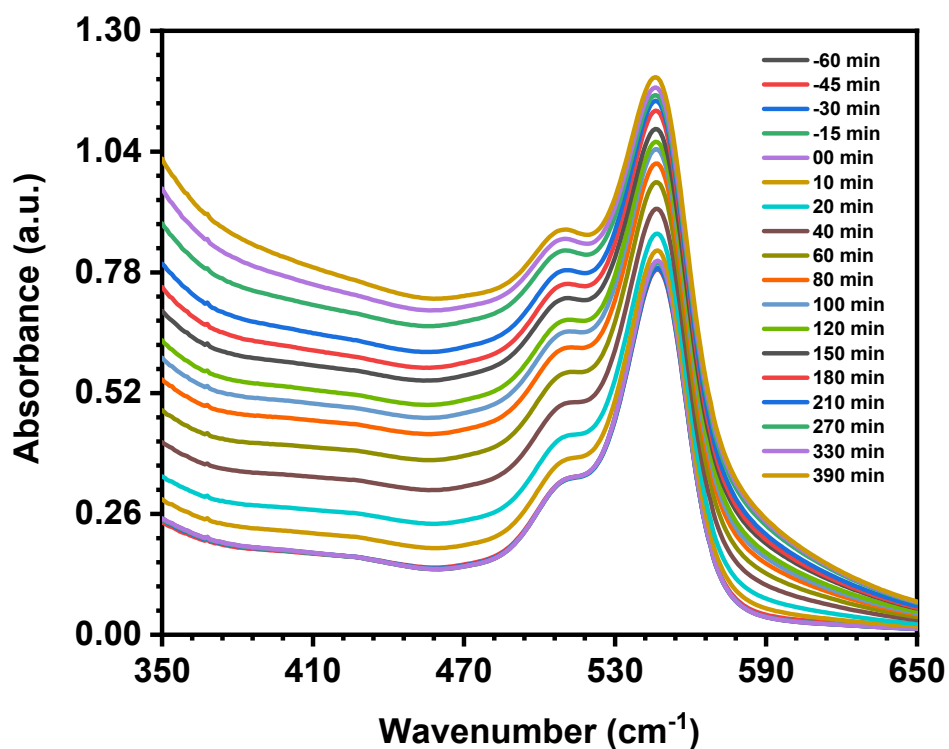


Figure S19. Photocatalytic degradation of RB at pH 7 catalyzed by CzTA-PDAN COP in presence of benzoquinone (BQ) as superoxide radical anion scavenger.

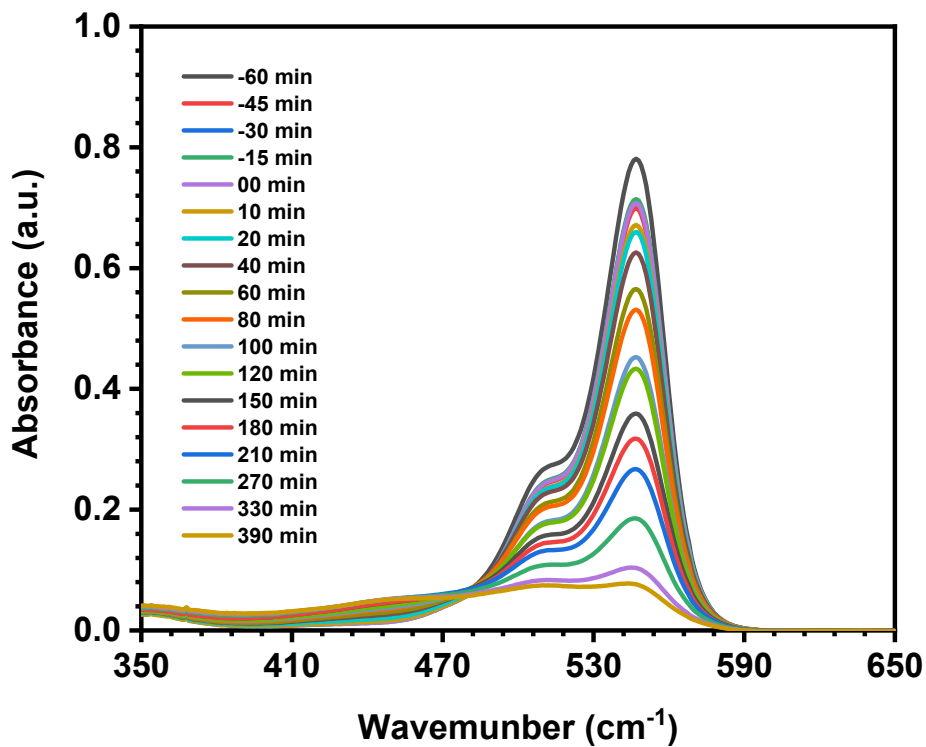


Figure S20. Photocatalytic degradation of RB at pH 7 catalyzed by CzTA-PDAN COP in the presence of sodium azide (NaN₃) as a singlet oxygen scavenger.

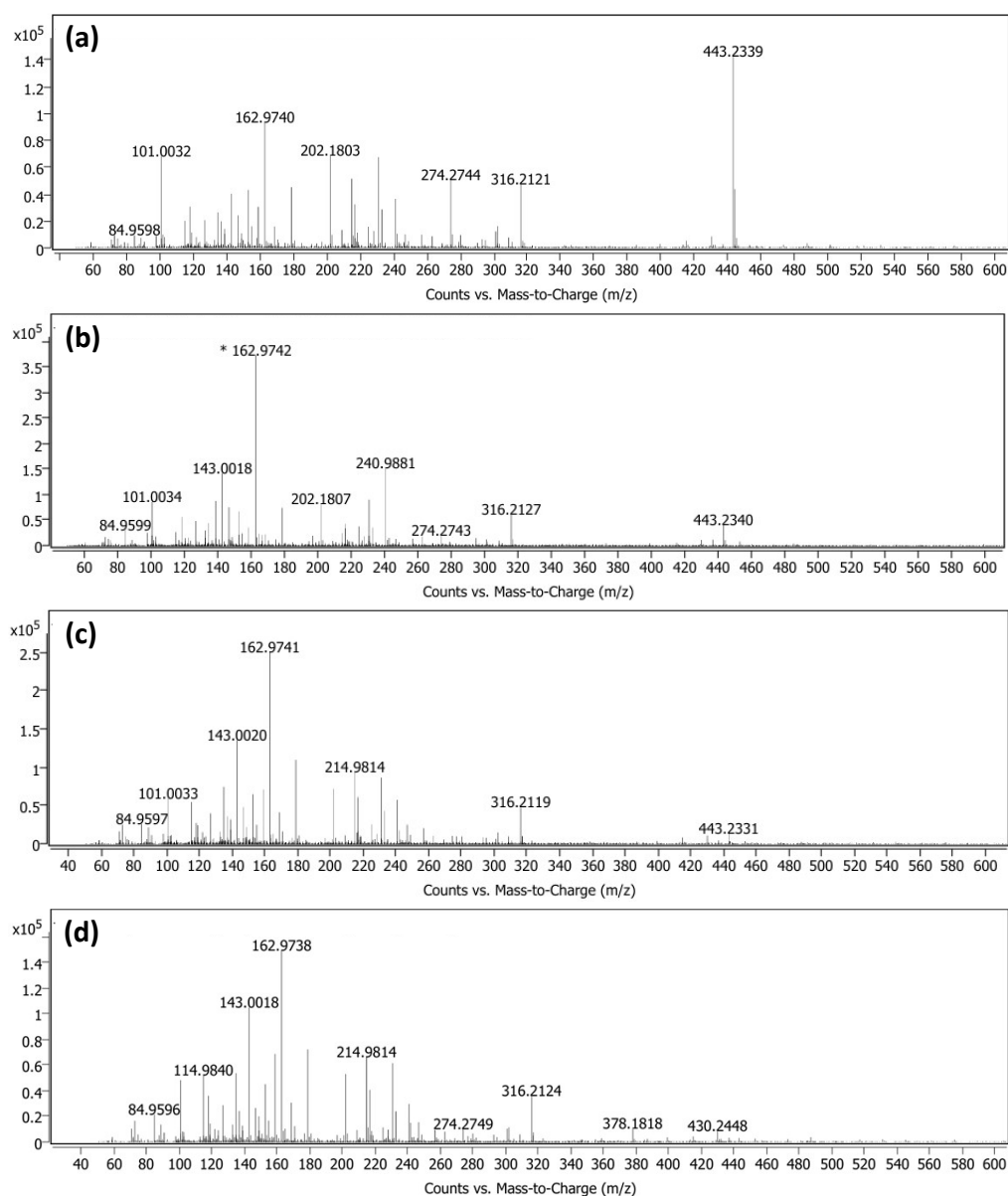
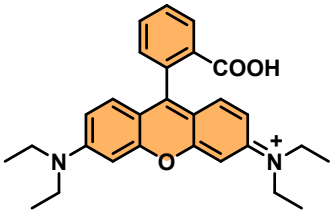
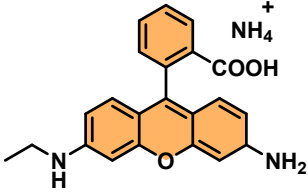
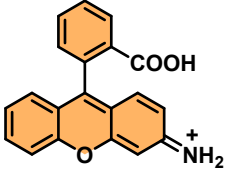
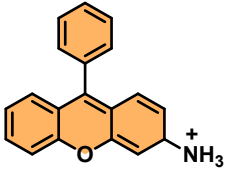
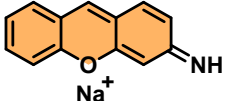
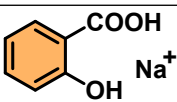
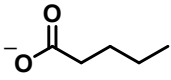
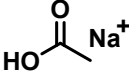
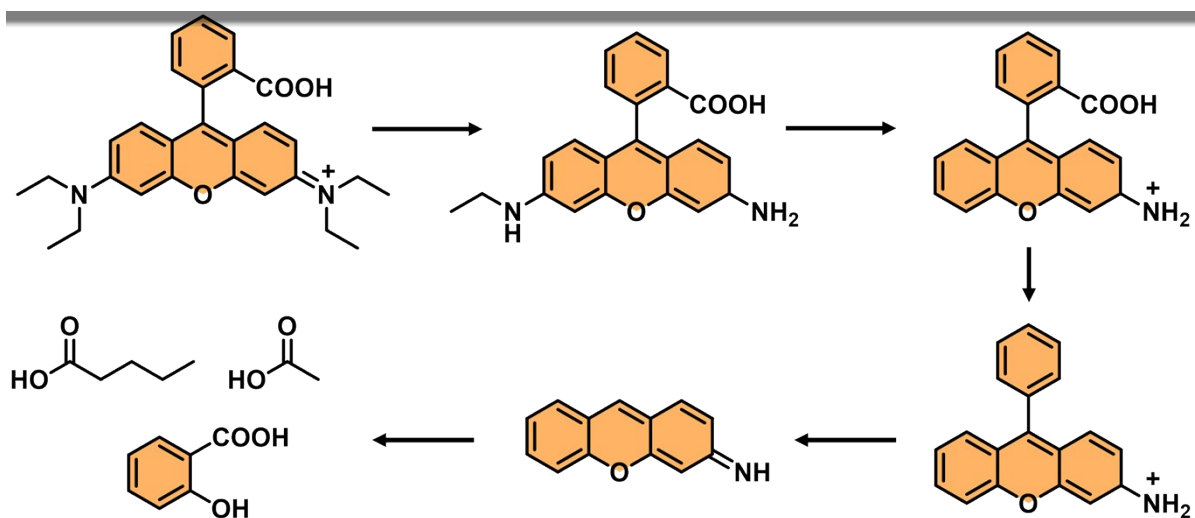


Figure S21. The HRMS spectra of the photodegradation products of RhB at different photodegradation times: (a) 0 min, (b) 20 min, (c) 40 min, and (d) 80 min in the presence of CzTA-PDAN COP.

Table S1. Detected intermediates of RhB degradation by CzTA-PDAN COP using HRMS.

Compound	Chemical formula	Molecular formula	Molecular weight
RhB		$C_{28}H_{31}N_2O_3^+$	443

1		$C_{22}H_{24}N_3O_3^+$	378
2		$C_{20}H_{14}NO_3^+$	316
3		$C_{19}H_{16}NO^+$	274
4		$C_{13}H_9NONa^+$	218
5		$C_7H_6O_3Na^+$	162
6		$C_5H_9O_2$	101
7		$C_2H_4O_2Na^+$	84



Scheme S5. Degradation pathway of RhB by CzTA-PDAN COP based on degradation intermediates detected by HRMS.

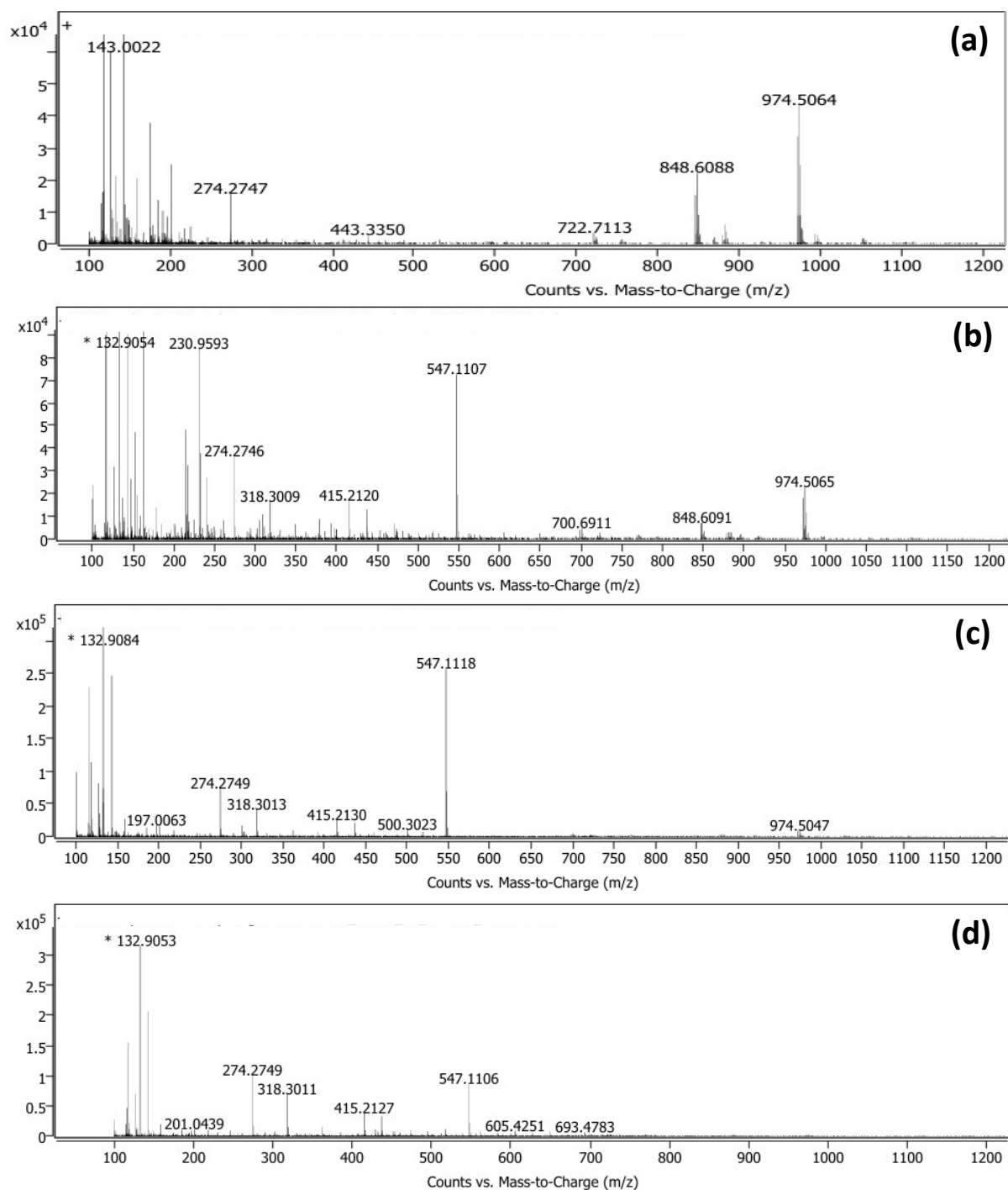
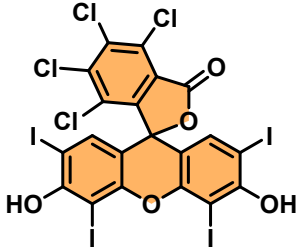
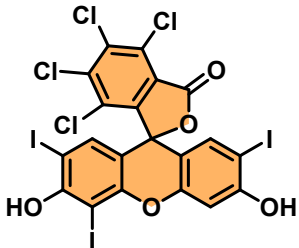
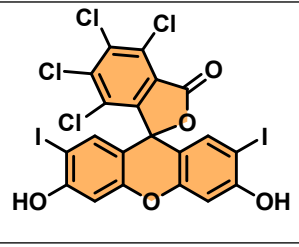
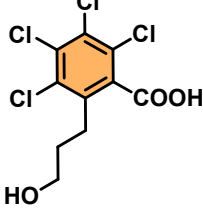
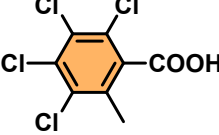
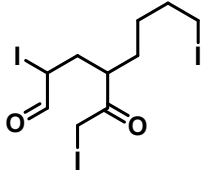
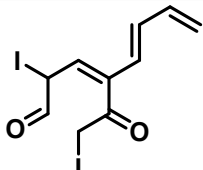
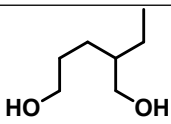


Figure S22. The HRMS spectra of the photodegradation products of RB at different photodegradation times: (a) 0 min, (b) 120 min, (c) 240 min, and (d) 360 min in the presence of CzTA-PDAN COP.

Table S2. Detected intermediates of RB degradation by CzTA-PDAN COP using HRMS.

Compound	Chemical formula	Molecular formula	Molecular weight
----------	------------------	-------------------	------------------

RB		$C_{20}H_4Cl_4I_4O_5$	974
1		$C_{20}H_4Cl_4I_3O_5$	848
2		$C_{20}H_4Cl_4I_2O_5$	722
3		$C_{10}H_8Cl_4O_3$	318
4		$C_8H_4Cl_4O_2$	274
5		$C_{10}H_{15}I_3O_2$	548
6		$C_{10}H_{10}I_2O_2$	416
7		$C_7H_{16}O_2$	132

POP-1(50 mg)	50 mL	10 mg/L	Visible light	30	45 (>99%)	⁶
POP-2 (50 mg)	50 mL	10 mg/L	Visible light	30	120(90%)	⁶
3Ph-CTF (10 mg)	50 mL	20 mg/L	UV-light	30	30 (>99%)	⁷
3Th-CTF (10 mg)	50 mL	20 mg/L	UV-light	30	45 (95%)	⁷
HDU-25 COF (2 mg)	50 mL	10 mg/L	Visible light	40	120 (>99%)	⁸
DA-CTF (8 mg)	40 mL	30 mg/L	Visible light	...	60 (92.33%)	⁹
HBD BTT (10 mg)	100 mL	10 mg/L	300 W Xenon lamp (>420 nm)	30	40 (>99%)	¹⁰
FBD BTT (10 mg)	100 mL	10 mg/L	300 W Xenon lamp (>420 nm)	30	30 (>99%)	¹⁰
CIBD BTT (10 mg)	100 mL	10 mg/L	300 W Xenon lamp (>420 nm)	30	30 (>99%)	¹⁰
TFP-TPTPh COF (7 mg)	56 mL	10 mg/L	Visible light	60	75 (>99%)	¹¹
BC-TT, BF-TT, and BIPE-TT CMPs (25 mg)	56 mL	20 mg/L for BC-TT CMP, 10 mg/L for both BF-TT and BIPE-TT CMPs	Visible light	60	90 (83%) for BC-TT CMP, 90 (63.7%) for BF-TT CMP and 90 (58%) for BIPE-TT CMP	¹²
CzTA-PDAN COP (10 mg)	50 mL	5 mg/L	White CFL and Sunlight	60	80 (>99%) in White CFL and 60 (>99%) in Sunlight	This work

Table S4. Catalytic performance of various types of photocatalysts for RB photodegradation.

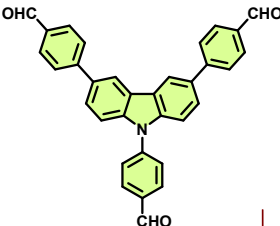
Photocatalyst (mg)	RB Dye solution (mL)	Conc. of RB Dye	Light source	Adsorption and desorption equilibrium (minute)	Light irradiation time (minute)	References
KA@CP-ARS (3 mg)	4 mL	10 mg/L	Sunlight	30	120 (96.54%)	¹³
ZnO (100 mg)	100 mL	30 mg/L	UV-light	30	60 (98%)	¹⁴
Zn-U3 (10 mg)	100 mL	5 mg/L	UV-light	60	4 h (94.87%)	¹⁵
PANI-Gr-3 wt% (200 mg)	100 mL	10 mg/L	Xenon arc lamp	180	3h (~56%)	¹⁶
CzTA-PDAN COP (10 mg)	50 mL	10 mg/L	White CFL	60	6.5 h (>99%)	This work

7. REFERENCES

1. R. P. Gaikwad, D. R. Naikwadi, A. V. Biradar and M. B. Gawande, *ACS Appl. Nano Mater.*, 2023, **6**, 1859-1869.
2. A. A. Yadav, S.-W. Kang and Y. M. Hunge, *J. Mater. Sci.: Mater. Electron.*, 2021, **32**, 15577-15585.
3. J. Yan, Z. Song, X. Wang, Y. Xu, W. Pu, H. Xu, S. Yuan and H. Li, *Appl. Surf. Sci.*, 2019, **466**, 70-77.
4. Z. Huang, M. Shen, J. Liu, J. Ye and T. Asefa, *J. Mater. Chem. A*, 2021, **9**, 14841-14850.
5. B. Chai, J. Yan, C. Wang, Z. Ren and Y. Zhu, *Appl. Surf. Sci.*, 2017, **391**, 376-383.
6. I. Nath, J. Chakraborty, P. M. Heynderickx and F. Verpoort, *Appl. Catal., B*, 2018, **227**, 102-113.
7. Y. Du, H. Ai, Y. Liu and H. Liu, *Sustainable Energy & Fuels*, 2023, **7**, 1747-1754.
8. W. Lu, C. Wang, Y. Han, Y. Bai, S. Wang, W. Xi and J. Wang, *Appl. Catal. A Gen.*, 2022, **647**, 118907.
9. Y. Zhuang, Q. Zhu, G. Li, Z. Wang, P. Zhan, C. Ren, Z. Si, S. Li, D. Cai and P. Qin, *Mater. Res. Bull.*, 2022, **146**, 111619.
10. C. Chu, Y. Qin, C. Ni and J. Zou, *Chin. Chem. Lett.*, 2022, **33**, 2736-2740.

11. J. H. Wang, T. A. Gaber, S. W. Kuo and A. F. M. EL-Mahdy, *Polym.*, 2023, **15**, 1685.
12. A. F. Saber, C.-C. Chueh, M. Rashad, S. W. Kuo and A. F. M. EL-Mahdy, *Mater. Today Sustain.*, 2023, **23**, 100429.
13. A. R. Sidar, M. Ahmad and K. A. Siddiqui, *Polyhedron*, 2023, **244**, 116605.
14. J. Kaur and S. Singhal, *Phys. B: Condens. Matter.*, 2014, **450**, 49-53.
15. F. A. Alharthi, A. Ali Alghamdi, H. S. Alanazi, A. A. Alsyahi and N. Ahmad, *Catalysts*, 2020, **10**, 1457.
16. S. Ameen, H. K. Seo, M. Shaheer Akhtar and H. S. Shin, *Chem. Eng. J.*, 2012, **210**, 220-228.

8. NMR DATA



monomer.

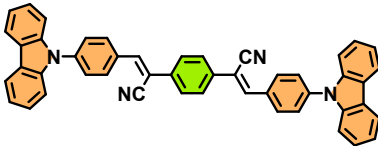


Figure S23. ^1H -NMR spectrum of Model compound-1.

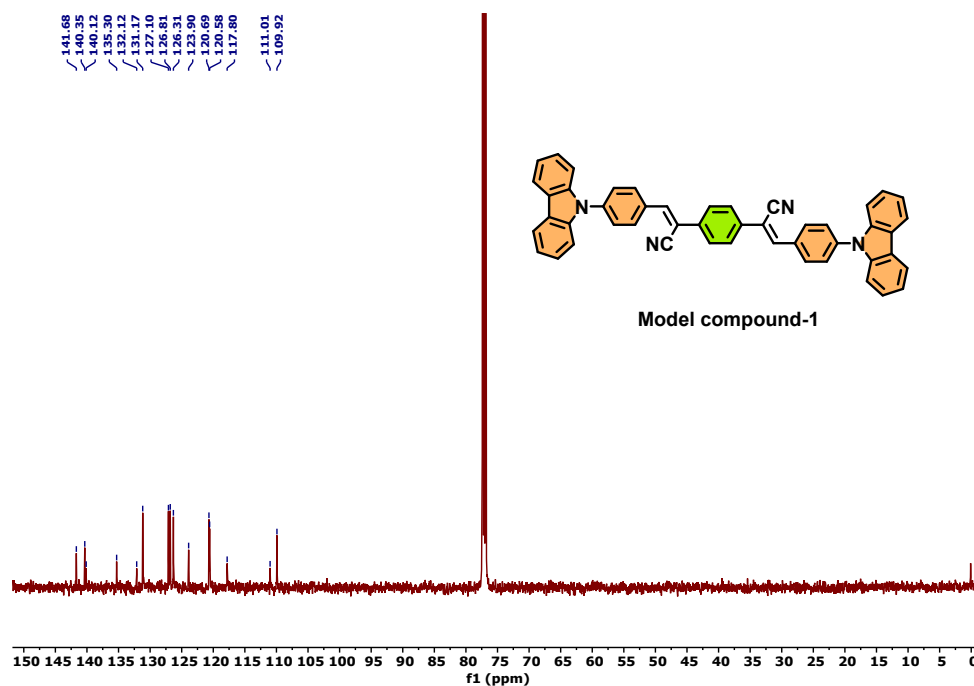


Figure S24. ¹³C-NMR spectrum of Model compound-1.

9. MALDI-TOF Mass Characterization

4,4',4''-(9*H*-carbazole-3,6,9-triyl)tribenzaldehyde (CzTA) has been characterized by MALDI-TOF mass spectra. The observed m/z values of $[M]^+$ or $[M+H]^+$ matched with the calculated m/z of the synthesized compound.

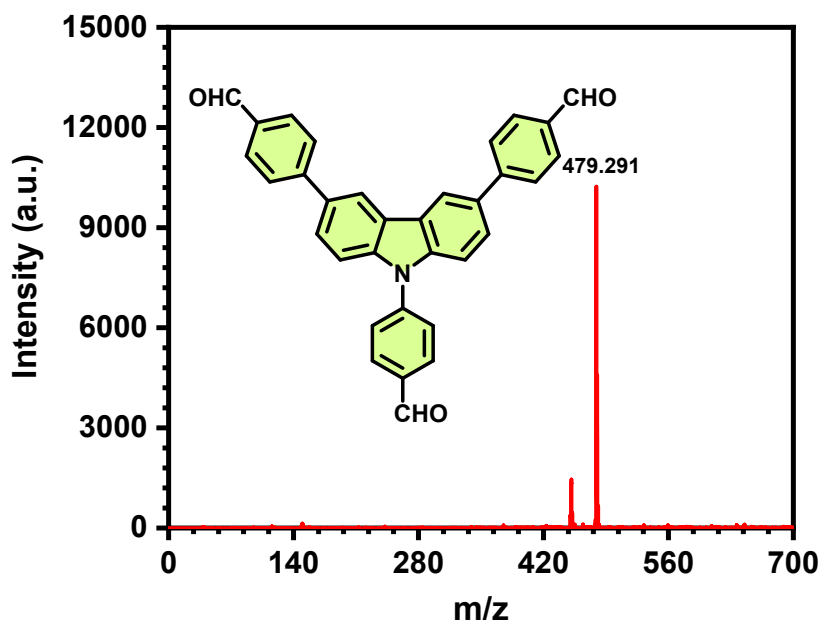


Figure S25. MALDI-TOF mass spectrum of 4,4',4''-(9*H*-carbazole-3,6,9-triyl)tribenzaldehyde (CzTA) monomer.